

Video Article

Disruption of Frontal Lobe Neural Synchrony During Cognitive Control by Alcohol Intoxication

Ksenija Marinkovic^{1,2}, Lauren E. Beaton¹, Burke Q. Rosen^{1,3}, Joseph P. Happer⁴, Laura C. Wagner¹¹Department of Psychology, San Diego State University²Department of Radiology, University of California San Diego³Department of Neurosciences, University of California San Diego⁴San Diego State University/UC San Diego Joint Doctoral Program in Clinical PsychologyCorrespondence to: Ksenija Marinkovic at kmarinkovic@sdsu.eduURL: <https://www.jove.com/video/58839>DOI: [doi:10.3791/58839](https://doi.org/10.3791/58839)

Keywords: Neuroscience, Issue 144, Neuroscience, brain, cognitive control, magnetoencephalography, theta oscillations, phase-locking, neural synchrony, alcohol, Stroop task, multimodal imaging

Date Published: 2/6/2019

Citation: Marinkovic, K., Beaton, L.E., Rosen, B.Q., Happer, J.P., Wagner, L.C. Disruption of Frontal Lobe Neural Synchrony During Cognitive Control by Alcohol Intoxication. *J. Vis. Exp.* (144), e58839, doi:10.3791/58839 (2019).

Abstract

Decision making relies on dynamic interactions of distributed, primarily frontal brain regions. Extensive evidence from functional magnetic resonance imaging (fMRI) studies indicates that the anterior cingulate (ACC) and the lateral prefrontal cortices (latPFC) are essential nodes subserving cognitive control. However, because of its limited temporal resolution, fMRI cannot accurately reflect the timing and nature of their presumed interplay. The present study combines distributed source modeling of the temporally precise magnetoencephalography (MEG) signal with structural MRI in the form of "brain movies" to: (1) estimate the cortical areas involved in cognitive control ("where"), (2) characterize their temporal sequence ("when"), and (3) quantify the oscillatory dynamics of their neural interactions in real time. Stroop interference was associated with greater event-related theta (4 - 7 Hz) power in the ACC during conflict detection followed by sustained sensitivity to cognitive demands in the ACC and latPFC during integration and response preparation. A phase-locking analysis revealed co-oscillatory interactions between these areas indicating their increased neural synchrony in theta band during conflict-inducing incongruous trials. These results confirm that theta oscillations are fundamental to long-range synchronization needed for integrating top-down influences during cognitive control. MEG reflects neural activity directly, which makes it suitable for pharmacological manipulations in contrast to fMRI that is sensitive to vasoactive confounds. In the present study, healthy social drinkers were given a moderate alcohol dose and placebo in a within-subject design. Acute intoxication attenuated theta power to Stroop conflict and dysregulated co-oscillations between the ACC and latPFC, confirming that alcohol is detrimental to neural synchrony subserving cognitive control. It interferes with goal-directed behavior that may result in deficient self-control, contributing to compulsive drinking. *In sum*, this method can provide insight into real-time interactions during cognitive processing and can characterize the selective sensitivity to pharmacological challenge across relevant neural networks.

Video Link

The video component of this article can be found at <https://www.jove.com/video/58839>

Introduction

The overall goal of this study is to examine the effects of acute alcohol intoxication on spatio-temporal changes in the brain oscillatory dynamics and long-range functional integration during cognitive control. The employed multimodal imaging approach combines magnetoencephalography (MEG) and structural magnetic resonance imaging (MRI) to provide insight into the neural basis of decision making with high temporal precision and at the level of an interactive system.

Flexible behavior makes it possible to adapt to changing contextual demands and to switch strategically between different tasks and requirements in agreement with one's intents and goals. The capacity to suppress automatic responses in favor of goal-relevant but non-habitual actions is an essential aspect of cognitive control. Extensive evidence suggests that it is subserved by a predominantly frontal cortical network, with the anterior cingulate cortex (ACC) as a central node in this interactive network^{1,2,3,4}. While the abundant anatomical connectivity between the ACC and lateral frontal cortices is well-described^{5,6}, the functional characteristics of communication between these regions during cognitive control, response selection and execution, are poorly understood.

The highly influential conflict monitoring theory^{7,8} proposes that cognitive control arises from a dynamic interaction between the medial and lateral prefrontal cortices. This account purports that the ACC monitors conflict between competing representations and engages the lateral prefrontal cortex (latPFC) to implement response control and optimize performance. However, this account is primarily based on the functional MRI (fMRI) studies using the blood oxygenation level dependent (BOLD) signal. The fMRI-BOLD signal is an excellent spatial mapping tool, but its temporal resolution is limited because it reflects regional hemodynamic changes mediated by neurovascular coupling. As a result, the BOLD signal changes unfold on a much slower time scale (in seconds) than the underlying neural events (in milliseconds)⁹. Moreover, the

BOLD signal is sensitive to alcohol's vasoactive effects¹⁰ and may not accurately represent the magnitude of neural changes, which makes it less suitable for studies of acute alcohol intoxication. Therefore, the presumed interplay between the medial and lateral prefrontal cortices and its sensitivity to alcohol intoxication need to be examined by methods that record neural events in a temporally precise manner. MEG has an excellent temporal resolution since it directly reflects postsynaptic currents. The anatomically-constrained MEG (aMEG) methodology employed here is a multimodal approach that combines distributed source modeling of the MEG signal with structural MRI. It allows for the estimation of *where* the conflict- and beverage-related brain oscillatory changes are occurring and to understand the temporal sequence (*"when"*) of the involved neural components.

Decision making relies on the interactions of distributed brain regions that are dynamically engaged to deal with increased demands on cognitive control. One way to estimate event-related changes in long-range synchrony between two cortical regions is to calculate their phase coupling as an index of their co-oscillations^{11,12}. The present study applied a phase-locking analysis to test the basic tenet of the conflict monitoring theory by examining the co-oscillatory interactions between the ACC and latPFC. Neural oscillations in theta range (4 - 7 Hz) are associated with cognitive control and have been proposed as a fundamental mechanism supporting the long-range synchronization needed for top-down cognitive processing^{13,14,15,16}. They are generated in prefrontal areas as a function of task difficulty and are significantly attenuated by acute alcohol intoxication^{17,18,19,20}.

Long-term excessive alcohol intake is associated with a range of cognitive deficits with prefrontal circuitry being especially affected^{21,22}. Acute alcohol intoxication is detrimental to cognitive control under conditions of increased difficulty, ambiguity, or those that induce response incompatibility^{17,23,24}. By affecting decision making, alcohol may interfere with goal-directed behavior, may result in poor self-control and increased drinking, and may also contribute to traffic- or work-related hazards^{25,26,27}. The present study uses an aMEG approach to measure the oscillatory activity in theta band and synchrony between the principal executive areas with excellent temporal resolution. The effects of alcohol on theta activity and co-oscillations between the ACC and the latPFC are examined as a function of conflict elicited by the Stroop interference task. We hypothesize that increased cognitive demands are associated with greater functional synchrony and that alcohol-induced dysregulation of synchronous activity of the medial and lateral prefrontal cortices underlies impairments in cognitive control.

Protocol

This experimental protocol has been approved by the Human Subjects Protection Committee at the University of California, San Diego.

1. Human Subjects

1. Recruit healthy right-handed adult volunteers, obtain their consent, and screen them on the inclusion/exclusion criteria.
NOTE: In this study, twenty young, healthy individuals (mean \pm standard deviation [SD] age = 25.3 \pm 4.4 years) including 8 women were recruited who drink in moderation, who have never been in treatment or arrested for drug or alcohol related offenses, who report no alcoholism-related symptoms on the Short Michigan Alcoholism Screening Test²⁸, who do not smoke nor use illegal substances, who do not have a history of neuropsychiatric disorders or any current health problems, and who are medication free and have no internal ferromagnetic objects or implants.

2. Experimental Design

1. Scan each participant four times, including three MEG sessions (a no-beverage introductory session and two experimental beverage sessions in which alcohol and placebo are administered in a counterbalanced manner), and one structural MRI scan.
NOTE: In this within-subject design, participants serve as their own controls by participating in both alcohol and placebo sessions. This design reduces error variance and increases statistical power by minimizing influence of individual variability in brain anatomy, activity patterns, and alcohol metabolism.

3. Collecting MEG Scans

1. **Perform familiarization session.**
 1. During the initial introductory session, administer questionnaires to obtain more information about the participants' medical history, their drinking patterns and severity of alcoholism-related symptoms^{28,29}, family history of alcoholism³⁰, and personality traits including impulsivity^{31,32}.
 2. Carry out an initial recording in the MEG scanner following the protocol described below in steps 3.2, 3.3, and 3.5. Do not provide any beverage. Explain the task and run the practice version allowing participants to get familiarized with it beforehand.
NOTE: The acclimation to the experimental situation serves the purpose of minimizing potential effects of situation-induced arousal³³, thereby equating subsequent alcohol and placebo sessions on that dimension.
2. **Perform the alcohol/placebo experimental sessions.**
NOTE: Follow the same experimental procedures during both alcohol and placebo sessions with the exception of the administered beverage. Counterbalance beverage order by administering alcohol beverage first to one half of participants and placebo to the other half in a random order.
 1. Upon their arrival to the MEG lab, run a brief test scan by putting the participant in the scanner and checking the channels for possible magnetization. Measure their weight. Screen them with an electronic breathalyzer. Query them about compliance with the requirements to abstain from alcohol for 48 h and from food for 3 h prior to the experiment.
 2. Collect urine samples for a multi-drug test panel from all participants and exclude those who test positive for any drug. In addition, check female participants for pregnancy with a urine test and exclude those who test positive or if they suspect that they might be pregnant.

3. Assess dynamic changes in the subjective effects of alcohol by asking participants to rate their momentary feelings and states on a standardized scale³⁴ prior to drinking and on two additional occasions during the experiment - on the ascending limb (~15 min after consuming beverage) and descending limb of the breath alcohol concentration curve (BrAC), after the MEG recording.
4. Administer a practice run of the Stroop task on a laptop with stimulus presentation software to ensure that the participants understand the task before recording.

NOTE: This version of the Stroop task combines reading and color naming (**Figure 1**). The congruent condition consists of color words (i.e., red, green, blue, yellow) that are printed in the matching font color (i.e., the word "green" is printed in green). In the incongruous condition, color words are printed in color that does not match their meaning (i.e., the word "green" is printed in yellow). Ask the participants to press one of four buttons corresponding to the font color whenever a word is written in color, or, when a word is written in gray, to press a button corresponding to the meaning of the word^{18,23}.
3. **Prepare the MEG/EEG recording.**

NOTE: Details of MEG data acquisition have been described in previous publications^{35,36,37}.

 1. Position the EEG cap or individual EEG electrodes on the head of the participant and check that all impedances are below 5 k Ω .
 2. Attach the head position indicator (HPI) coils on either side of the forehead and behind each ear.

NOTE: This step is specific to Neuromag systems.
 3. Digitize positions of the fiducial points including the nasion and two preauricular points, positions of HPI coils, EEG electrodes, and obtain a large number of additional points (~200) delineating the head shape. Use this information for the co-registration with anatomical MRI images (**Figure 2**).
4. **Administer beverage.**
 1. Prepare alcohol beverage by mixing premium quality vodka with chilled orange juice (25% v/v), based on each participant's gender and weight (0.60 g/kg alcohol for men, 0.55 g/kg alcohol for women), targeting a BrAC of 0.06%³⁸. Serve the same volume of orange juice in glasses with rims swabbed with vodka as a placebo beverage. Ask the participant to consume the beverage in approximately 10 min.
 2. Check the participants' BrAC with the breathalyzer starting at ~15 min after drinking and then every 5 min until they enter the recording chamber. Since electronic devices cannot be used in the shielded room, use a saliva alcohol test, which consists of a cotton swab that is saturated in saliva and is inserted into a receptacle that provides a readout.
5. **Acquire MEG/EEG data.**
 1. Position the participant comfortably in the scanner. Since the prefrontal activity is of particular interest, ensure that the participant is positioned so that his/her head is touching the top of the helmet and is aligned along the front.

NOTE: Head position can affect activity estimates in significant ways because the magnetic field gradients decrease with the cube of the distance between the sensors and the brain sources³⁹.
 2. Connect HPI coils and all of the electrodes to their respective inputs on the scanner. Position response pads so that the buttons can be pressed comfortably. Ascertain that the font is clearly legible on the projection screen in front of the participant.
 3. Back in the console room, check that the intercom is functioning properly. Remind the participant to minimize blinking and to avoid movements including head motion caused by talking. Instruct the participant to reply to questions by pressing response buttons instead.
 4. Check that all response and stimulus triggers are recorded correctly. Examine all channels for artifacts and measure the head position in the scanner.
 5. Start data acquisition and begin the task. Give breaks every ~2.5 min to rest the eyes. Save the data upon task completion and escort the participant out of the recording chamber.
 6. When the participant has exited the scanner, acquire approximately two minutes of data from the empty room as a measure of instrumental noise.
 7. Ask the participant to rate perceived task difficulty, content of the imbibed beverage, how intoxicated they felt, as well as their momentary moods and feelings³⁴.

4. Image Acquisition and Cortical Reconstruction of Structural MRI

1. Obtain a high-resolution anatomical MRI scan for each participant, and reconstruct each participant's cortical surface with FreeSurfer software^{40,41,42}.
2. Use the inner skull surface derived from the segmented structural MRI images to generate a boundary element model of the volume conductor, which is used to provide a model for the forward solution that is consistent with each individual's brain anatomy^{43,44}.

5. MEG Data Analysis

NOTE: Analyze the data with the anatomically-constrained MEG approach which uses each participant's reconstructed cortical surface to constrain source estimates to the cortical ribbon^{40,45,46}. The analysis stream relies on custom functions with dependencies on publicly available packages including FieldTrip⁴⁷, EEGLab⁴⁸, and MNE⁴⁹.

1. During data preprocessing, use a permissive band-pass filter (e.g., 0.1 - 100 Hz) and epoch data with respect to stimulus onset into segments that include padding intervals on each end (e.g., -600 to 1100 ms for an interval of interest spanning -300 to 800 ms after the removal of padding).
2. Remove noisy and flat channels, as well as trials containing artifacts by visual inspection and using threshold-based rejection. Use independent component analysis⁴⁸ to remove eyeblink and heartbeat artifacts. Eliminate trials with incorrect responses.
3. Apply Morlet wavelets (**Figure 3**)⁴⁷ to calculate complex power spectrum for each trial in 1 Hz increments for theta frequency band (4 - 7 Hz). Remove any additional artifacts. Compute the noise covariance from empty room data.
4. **Co-register the MEG data with MRI images using the three-dimensional (3D) head digitization information (Figure 2).**

1. Open the MRILab module.
 2. Select **File| Open| Select subject's structural MRI**.
 3. Select **File| Import| Isotrak data| select raw data.fif file| Make Points**.
 4. Select **Windows| Landmarks| Adjust fiducial landmarks** until co-registration of MEG data and MRI are acceptable.
 5. Select **File| Save**.
5. Calculate noise-sensitivity normalized estimates of theta source power and phase with a spectral dynamic statistical mapping approach^{18,50}. Express event-related theta source power as percent signal change relative to baseline.
 6. Create group averages of event-related theta source power by morphing each participant's estimates onto an average cortical representation⁵¹.
 7. **Visualize the source estimates on an inflated average surface to enhance visibility of sulcal estimates (Figure 4).**
 1. Open the MNE software.
 2. Select **File| Load Surface| Load inflated group-average FreeSurfer cortical surface**.
 3. Select **File| Manage overlays| Load stc| Load group-averaged data| Select loaded file from available overlays**.
 4. Select overlay type as **Other**.
 5. Adjust **Color Scale thresholding| Show**.
 6. View **brain movies** and examine spatio-temporal stages of processing by identifying areas and time windows characterized by highest activation.
 8. Create unbiased regions of interest (ROIs) based on overall group-averaged estimates to incorporate cortical locations with most notable source power. Calculate time courses for each subject, condition, and ROI (**Figure 5**).
 9. **Submit the obtained theta source power estimates to the statistical analysis.**
 1. Extract time windows of interest from each ROI time course and perform analysis of variance (ANOVA) with beverage (alcohol, placebo) and trial type (congruous, incongruous) as within subject factors. Use a nonparametric cluster-based permutation test⁵² to examine beverage and condition comparisons of event-related theta power as well as phase-locking values (PLV).
 10. Estimate task-related changes in the long-range synchronization between the main activation foci in the ACC and the latPFC by computing the PLV¹². Express PLV as percent change relative to baseline.

NOTE: The PLV is an indicator of consistency of the phase angle between the two ROIs across trials as it measures the extent to which they co-oscillate at a particular frequency and in real time (**Movie 1**).
 11. Calculate correlations between ROI MEG activity estimates, indices of behavioral performance, and questionnaire scores to inform interpretation of the observed results.

Representative Results

Behavioral results indicate that the Stroop task successfully manipulated response interference because the accuracy was the lowest and the response times the longest on incongruous trials (**Figure 6**). Alcohol intoxication lowered accuracy but did not affect reaction times¹⁸.

The spatio-temporal sequence of activity in theta frequency band revealed with the aMEG approach is overall in agreement with generally accepted models of cognitive functions in this type of task. As illustrated in the brain movies (**Movie 2**), the visual cortex is activated at around 100 ms after stimulus onset, followed by a posterior-to-anterior activation pattern that engages primarily frontal cortices during cognitive integration stages after ~300 ms. The ACC is particularly sensitive to incongruous (INC), high-conflict trials, indicating its engagement during conflict monitoring. The ACC is the principal generator of theta oscillations during tasks probing cognitive control but the latPFC is also active during the integration stage at around 350-600 ms. Activation of the motor cortex is visible after ~600 ms during the response preparation stage (**Movie 2B**). Event-related theta power is greatest on INC trials, which is consistent with its sensitivity to conflict demands (**Figure 5**), especially in the prefrontal cortex^{13,17,19,20}. Theta power is decreased by acute alcohol intoxication overall. However, when compared to congruous (CONG) trials, alcohol decreases theta power on INC (high conflict) trials selectively in the ACC and latPFC¹⁸.

The present study extends the results from Kovacevic et al.¹⁸ by focusing on dynamic interactions between these areas during the processing of Stroop interference in light of a prevailing account of the cognitive control network^{7,8}. To better understand the timing, degree, and nature of the interactions between these two principally engaged cortical areas, the PLVs were calculated for each beverage and task condition, and for each participant. As shown in a group average in **Figure 7**, co-oscillations between the ACC and latPFC vary across time with an overall early increase in co-oscillations during a stimulus processing stage. Under placebo, this is followed by a sustained increase after ~400 ms on incongruous trials during the integration and response preparation stage. Thus, synchronized co-oscillations between the medial and lateral prefrontal cortices are observed only on the more difficult, INC trials evoking response conflict $F(1,19) = 5.5, p < 0.05$. This evidence supports the proposal that the ACC and the latPFC functionally interact in real time to subserve cognitive control. In contrast, acute alcohol intoxication significantly dysregulates the co-oscillations, yielding a Condition x Beverage interaction, $F(1,19) = 5.1, p < 0.05$, in which incongruous trials specifically were affected by alcohol $F(1,19) = 8.8, p < 0.01$ (**Figure 7**). This may underlie alcohol-induced impairments of inhibitory control and indicates the vulnerability of top-down regulative functions of the prefrontal cortex to acute intoxication.

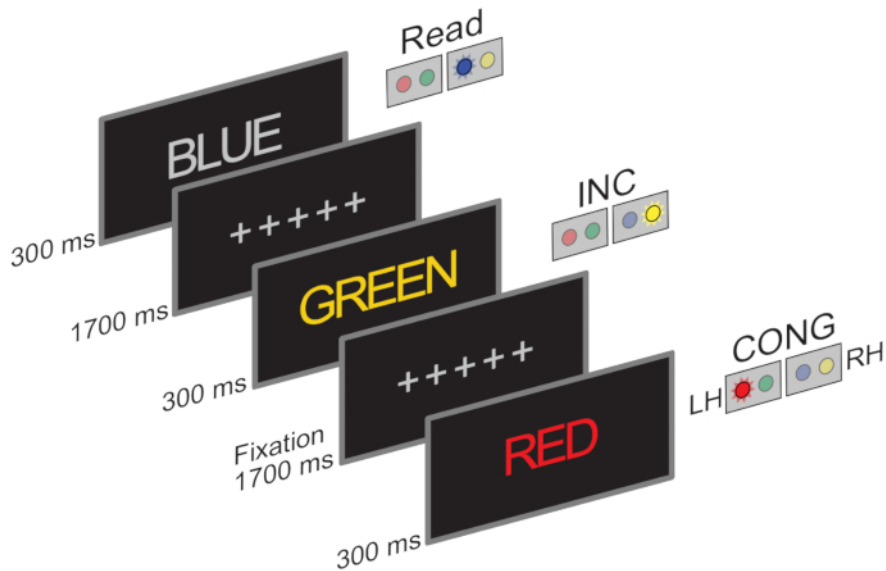


Figure 1: Stroop task combines color naming and reading. Trial examples for each of the three conditions along with the correct response color are presented. In the congruous condition (CONG), font color is consistent with the word meaning, while incongruous trials (INC) trials elicit response conflict due to interference from word meaning. Participants are instructed to press a button corresponding to the font color when words are written in color (CONG, INC) and to respond to the word meaning (Read) when they are written in gray. Trials are presented for 300 ms and then replaced by a fixation screen for 1700 ms. Trial types are presented in a randomized order. In this particular version, the CONG and INC conditions were equiprobable and were presented on 16.7% trials each out of 576 trials total. [Please click here to view a larger version of this figure.](#)

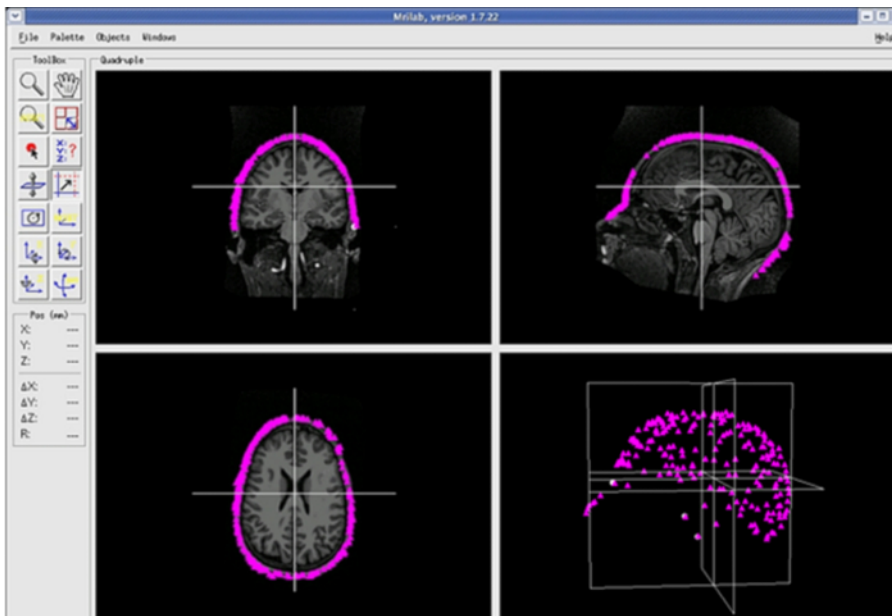


Figure 2: Co-registration of MEG and MRI. Digitized points across the head collected during the MEG recording are used for co-registration with anatomical MRI images. [Please click here to view a larger version of this figure.](#)

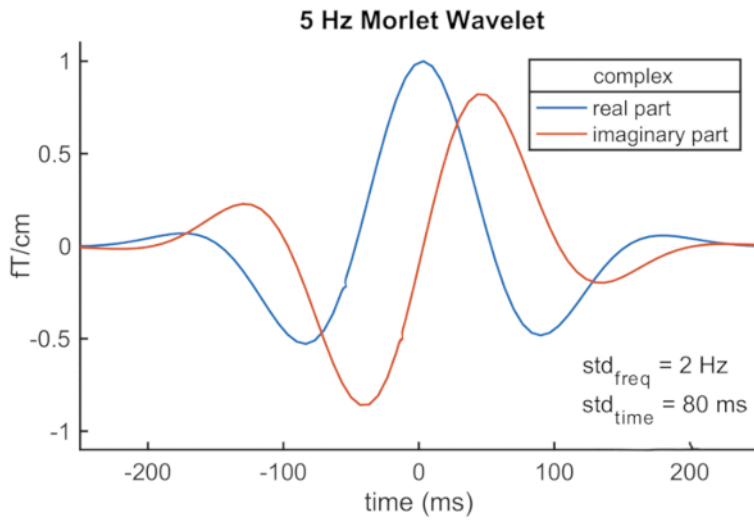


Figure 3: Morlet wavelet. Morlet wavelets are used to calculate complex power spectrum for each trial in 1 Hz frequency increments for the theta band frequency (4 - 7 Hz). [Please click here to view a larger version of this figure.](#)



Figure 4: Cortical reconstruction and inflation. Individual cortical surfaces are reconstructed and are used to constrain estimated source power. Here shown is an average cortical surface which is inflated to enhance visibility of the sources estimated to cortical sulci. [Please click here to view a larger version of this figure.](#)

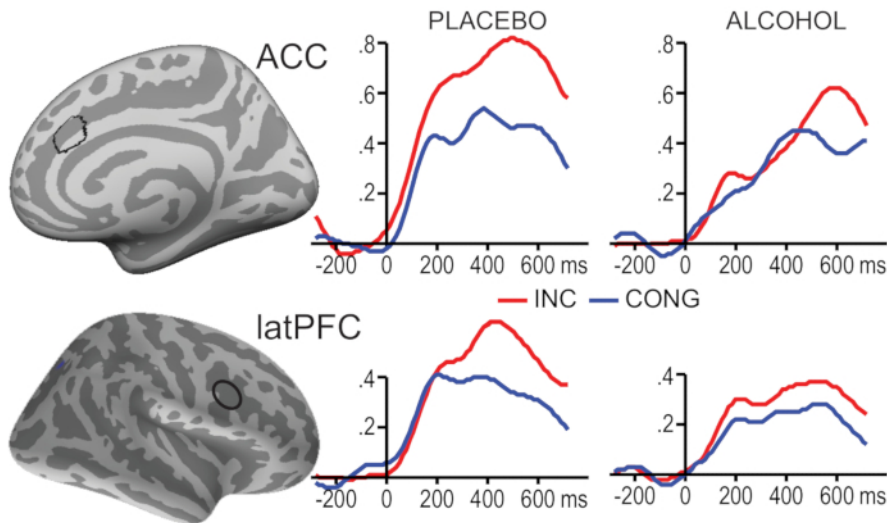


Figure 5: Group-average time courses of event-related theta source power estimates in selected regions of interest. Incongruous (INC) stimuli elicited increased event-related theta power compared to congruous (CONG) stimuli in the anterior cingulate cortex (ACC; $F(1,19) = 34.1$, $p < 0.0001$) as well as the lateral prefrontal cortex (latPFC; $F(1,19) = 11.0$, $p < 0.01$), during 480 - 670 ms. Conflict processing is particularly sensitive to alcohol intoxication as theta power to INC was attenuated by alcohol intoxication ($F(1,19) = 9.9$, $p < 0.01$). The y-axis depicts baseline-corrected noise-normalized event-related theta source power. This figure has been modified from Kovacevic et al.¹⁸. [Please click here to view a larger version of this figure.](#)

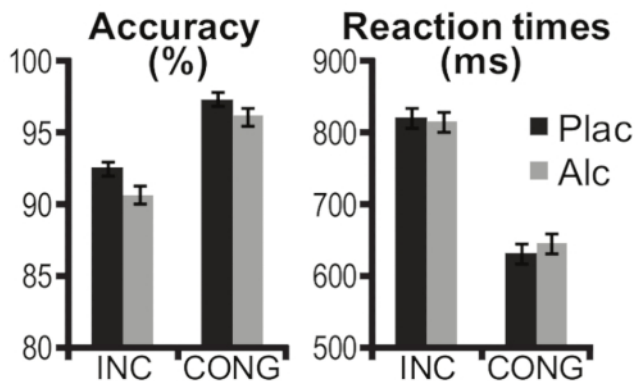


Figure 6: Behavioral results on the Stroop task. Stroop interference was reflected in decreased accuracy and longer response times to incongruous (INC) trials. Alcohol intoxication (Alc) impaired accuracy compared to placebo (Plac) but did not affect reaction times. Error bars signify standard error of the mean. This figure has been modified from Kovacevic et al.¹⁸. [Please click here to view a larger version of this figure.](#)

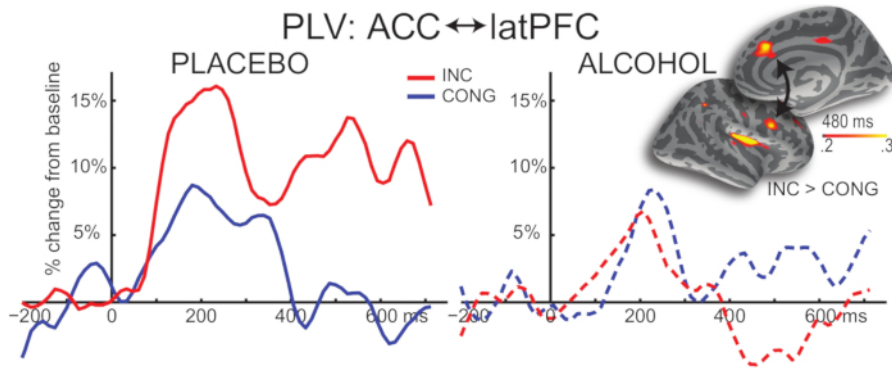
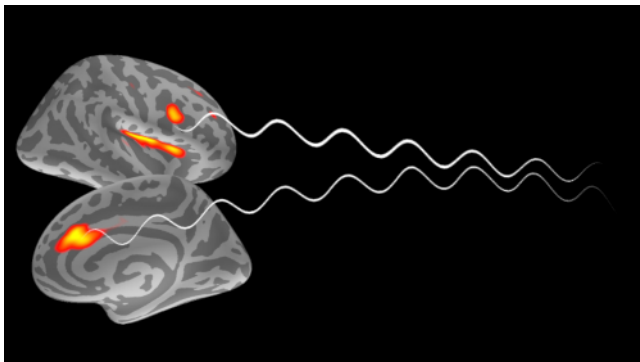
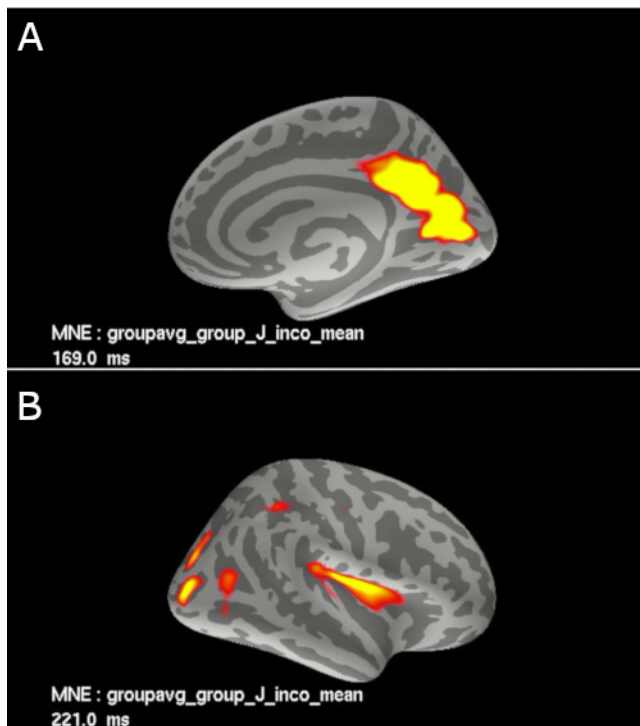


Figure 7: Group-average time courses of phase-locking values (PLVs) in the theta band. Co-oscillatory synchrony between the anterior cingulate cortex (ACC) and lateral prefrontal cortex (latPFC) in theta band expressed as percent change from baseline for placebo (left) and alcohol (right) conditions. Following an early increase in PLVs during a stimulus processing stage (400 - 600 ms), a sustained increase in co-oscillations is observed on incongruous (INC) trials in response to increased cognitive control compared to congruous (CONG) trails under placebo, $F(1,19) = 5.5, p < 0.05$. Acute alcohol intoxication selectively dysregulated the co-oscillations on INC trials, $F(1,19) = 8.8, p < 0.01$. Activation maps (inset) show the incongruity effect (INC-CONG), which is prominent in the ACC and latPFC. The color scale denotes baseline-corrected source power estimates at 480 ms after stimulus onset, with red (activity > 0.2) to yellow (activity > 0.3) indicating stronger theta power to INC trials compared to CONG trials. [Please click here to view a larger version of this figure.](#)



Movie 1: Co-oscillations. Phase-locking values were calculated in the theta frequency range (4 - 7 Hz) between the anterior cingulate cortex (ACC) and lateral prefrontal cortex (latPFC) as a measure of synchronization that is sensitive to the consistency of the phase difference between these two ROIs regardless of their theta power amplitude. [Please click here to download this movie.](#)



Movie 2: Brain movies. Distributed source modeling of the MEG signal combined with structural MRI allows for the estimation of principal cortical areas generating theta power and the temporal sequence of their activation in response to the Stroop interference. **(A)** Following early sensory processing, the anterior cingulate cortex (ACC) is selectively activated by incongruous, high-conflict trials after ~350 ms. **(B)** While the ACC is the principal generator of theta oscillations during tasks probing cognitive control, the lateral prefrontal cortex (latPFC) is also engaged during the integration stage around 350 - 600 ms. Activation of the motor cortex is observed after ~600 ms during response preparation. The color scale denotes differential baseline-corrected source power estimates, with red color indicating activation greater than 0.79 medially (0.57 laterally) and yellow indicates activation greater than 0.9 medially (0.8 laterally). Please note that these two movies should be shown together with unfolding time courses pertaining to the ACC and latPFC, respectively. [Please click here to download these movies.](#)

Discussion

The multimodal imaging method used in this study comprises distributed source modeling of the temporally precise MEG signal along with spatial constraints of inverse estimates derived from each participant's structural MRI. The aMEG approach combines the strengths of these techniques to provide insight into the spatio-temporal stages of oscillatory dynamics and the long-range integration subserving cognitive control. This method provides greater temporal precision than other neuroimaging techniques such as fMRI-BOLD whose temporal resolution is on the magnitude of seconds due to its indirect sensitivity to neural changes via neurovascular coupling⁹. In comparison, the millisecond precision of MEG signal allows for the investigation of neural processing stages, as demonstrated by the present study. The aMEG model assumes distributed sources of the MEG signal along the cortical surface which, when reconstructed from structural MRI images, provides spatial constraints for activity estimates^{45,53}. These spatial estimates can be used to investigate not only local activation but long-range communication at an interactive network level in the form of phase-locking^{16,20}. Moreover, the aMEG approach is well suited for investigating the effects of pharmacological manipulation on neural functions, given that the fMRI-BOLD signal is confounded by the vasoactive effects of pharmacological manipulations such as alcohol and may not accurately reflect the magnitude of neural changes¹⁰.

The high sensitivity of this method to minute neural changes means that it is also sensitive to non-neural noise including muscle movements or eye blinks, so the various artifacts need to be detected and carefully removed from the raw signal. Moreover, head position can have significant effects on activity estimates due to sensor sensitivity to magnetic field gradients³⁹. Given the assumptions of the aMEG model, source estimates are constrained to the cortical surface^{45,46}, so the activity elicited from subcortical structures cannot be estimated.

Based on previously published results¹⁸, the present study has illustrated changes in event-related theta (4 - 7 Hz) power during Stroop-induced conflict as a function of acute alcohol intoxication in healthy social drinkers. As shown in **Figure 5**, theta power is differentially sensitive to cognitive demands imposed by the Stroop task conditions. Incongruity is especially effective in engaging cognitive control as reflected in greater theta power in the prefrontal cortex compared to prestimulus baseline. The principal estimated generator of theta oscillations is the ACC that is sensitive to response conflict during both early and late processing stages¹⁸. These findings support the role of the ACC in monitoring for conflict in concordance with prominent accounts^{7,8}. Thus, the aMEG method has provided a temporally-sensitive insight into the sustained engagement of the ACC during trials imposing higher load on cognitive control. Together with extensive anatomical connections between the ACC and distributed brain regions^{5,6}, this evidence corroborates its multifaceted role in self-regulation. On that view, the ACC is a key hub in the neurofunctional system that subserves cognitive control by aligning goals and intentions with contextual and motivational constraints^{54,55}. Inferolateral prefrontal cortex, especially on the right, is another important area within that system which has been associated with inhibition of prepotent responses, attentional control, and working memory in the service of updating task representations^{56,57,58}.

It has been established that theta oscillations mediate neural integration necessary for cognitive and affective processing^{13,16,59,60}. Neural communication may thus rely on synchronized excitability of distant neuronal ensembles in theta band with nested fast rhythms mediating local processing^{61,62}. PLVs reflect phase consistency between cortical areas and are commonly used to estimate their oscillatory synchrony as it is assumed that two areas interact when they co-oscillate⁶³. Indeed, transient increases in PLV are observed in those intervals of neural activity that would be expected to necessitate synchronous interactions^{12,20}. The present study confirms previous evidence and adds spatio-temporal refinement to the functional synchronization between the sources estimated to the ACC and the latPFC. Consistent with previous reports⁶⁴, the present results indicate that PLVs are increased and sustained on incongruous trials in the Stroop task. By quantifying phase synchronization between these two areas with high temporal precision, these findings extend the conflict monitoring account and indicate that their interaction is particularly prominent after ~350 ms on incongruous trials. During this cognitive integration stage, the medial and lateral prefrontal cortices are likely to interact to support behavioral performance during more difficult task conditions imposing demands on attention, response inhibition, and working memory. Extensive evidence from fMRI-based functional connectivity studies indicates that these cortical areas form a dynamic, interactive cingulo-opercular network that supports top-down cognitive control^{65,66,67}. More broadly, the brain optimizes responding to environmental demands in an adaptive and coherent manner via flexible and dynamic synchronization of distributed neurofunctional systems^{68,69}.

The anatomically-constrained MEG approach used in the present study relies on a combination of complementary imaging methods. It can characterize the spatio-temporal sequence of neural activity and can provide insight into the dynamics of long-range interactions important for integrating top-down influences during engagement of cognitive control. The MEG signal reflects synaptic currents directly, which allows for testing hypotheses about co-oscillatory interactions within and across neurofunctional systems with high temporal precision. Furthermore, this method is suitable for pharmacological manipulations because it is not susceptible to vasoactive confounds. Research from this lab and others indicates that prefrontally-mediated cognitive control functions are particularly vulnerable to alcohol intoxication^{17,18,19,20,23,24,70,71,72,73,74}. The present study shows that acute alcohol intoxication decreases activity in the prefrontal areas subserving response conflict. Furthermore, alcohol disrupts synchronized co-oscillations^{20,75} that may underlie impaired or maladaptive response suppression. As a result, intoxicated individuals exhibit deficient self-control resulting in disinhibition which may contribute to compulsive drinking and the development of alcohol dependence^{25,26,76}. In sum, estimates of synchronous co-oscillations can illuminate real-time interactions of the neural systems engaged by a particular cognitive demand and can inform a realistic brain-based model. They can characterize the selective sensitivity to alcohol challenge across networks and serve as biomarkers of individual vulnerability to pharmacological effects.

Disclosures

The authors have nothing to disclose.

Acknowledgments

This work has been supported by the National Institutes of Health (R01-AA016624). We are grateful to Dr. Sanja Kovacevic for her important contributions.

References

- Ridderinkhof, K. R., van den Wildenberg, W. P., Segalowitz, S. J., Carter, C. S. Neurocognitive mechanisms of cognitive control: the role of prefrontal cortex in action selection, response inhibition, performance monitoring, and reward-based learning. *Brain and Cognition*. **56** (2), 129-140 (2004).
- Shenhav, A., Cohen, J. D., Botvinick, M. M. Dorsal anterior cingulate cortex and the value of control. *Nature Neuroscience*. **19** (10), 1286-1291 (2016).
- Walton, M. E., Croxson, P. L., Behrens, T. E., Kennerley, S. W., Rushworth, M. F. Adaptive decision making and value in the anterior cingulate cortex. *Neuroimage*. **36 Suppl 2**, T142-154 (2007).
- Heilbronner, S. R., Hayden, B. Y. Dorsal Anterior Cingulate Cortex: A Bottom-Up View. *Annual Review of Neuroscience*. **39** 149-170 (2016).
- Barbas, H. Connections underlying the synthesis of cognition, memory, and emotion in primate prefrontal cortices. *Brain Research Bulletin*. **52** (5), 319-330 (2000).
- Morecraft, R. J., Tanji, J. in *Cingulate neurobiology and disease*. (ed B. A. Vogt) 114-144 Oxford University Press (2009).
- Botvinick, M. M. Conflict monitoring and decision making: reconciling two perspectives on anterior cingulate function. *Cognitive, Affective, & Behavioral Neuroscience*. **7** (4), 356-366 (2007).
- Carter, C. S., van Veen, V. Anterior cingulate cortex and conflict detection: an update of theory and data. *Cognitive, Affective, & Behavioral Neuroscience*. **7** (4), 367-379 (2007).
- Buxton, R. B. *Introduction to Functional Magnetic Resonance Imaging*. Cambridge University Press, New York, NY (2002).
- Rickenbacher, E., Greve, D. N., Azma, S., Pfeuffer, J., Marinkovic, K. Effects of alcohol intoxication and gender on cerebral perfusion: an arterial spin labeling study. *Alcohol*. **45** (8), 725-737 (2011).
- Fell, J., Axmacher, N. The role of phase synchronization in memory processes. *Nature Reviews Neuroscience*. **12** (2), 105-118 (2011).
- Lachaux, J. P., Rodriguez, E., Martinerie, J., Varela, F. J. Measuring phase synchrony in brain signals. *Human Brain Mapping*. **8** (4), 194-208 (1999).
- Cavanagh, J. F., Frank, M. J. Frontal theta as a mechanism for cognitive control. *Trends in Cognitive Sciences*. **18** (8), 414-421 (2014).
- Sauseng, P., Griesmayr, B., Freunberger, R., Klimesch, W. Control mechanisms in working memory: a possible function of EEG theta oscillations. *Neuroscience & Biobehavioral Reviews*. **34** (7), 1015-1022 (2010).
- Wang, C., Ulbert, I., Schomer, D. L., Marinkovic, K., Halgren, E. Responses of human anterior cingulate cortex microdomains to error detection, conflict monitoring, stimulus-response mapping, familiarity, and orienting. *The Journal of Neuroscience*. **25** (3), 604-613 (2005).
- Halgren, E. et al. Laminar profile of spontaneous and evoked theta: Rhythmic modulation of cortical processing during word integration. *Neuropsychologia*. **76** 108-124 (2015).

17. Rosen, B. Q., Padovan, N., Marinkovic, K. Alcohol hits you when it is hard: Intoxication, task difficulty, and theta brain oscillations. *Alcoholism: Clinical and Experimental Research*. **40** (4), 743-752 (2016).
18. Kovacevic, S. *et al*. Theta oscillations are sensitive to both early and late conflict processing stages: effects of alcohol intoxication. *PLoS One*. **7** (8), e43957 (2012).
19. Marinkovic, K., Rosen, B. Q., Cox, B., Kovacevic, S. Event-related theta power during lexical-semantic retrieval and decision conflict is modulated by alcohol intoxication: Anatomically-constrained MEG. *Frontiers in Psychology*. **3** (121) (2012).
20. Beaton, L. E., Azma, S., Marinkovic, K. When the brain changes its mind: Oscillatory dynamics of conflict processing and response switching in a flanker task during alcohol challenge. *PLoS One*. **13** (1), e0191200 (2018).
21. Oscar-Berman, M., Marinkovic, K. Alcohol: effects on neurobehavioral functions and the brain. *Neuropsychology Review*. **17** (3), 239-257 (2007).
22. Le Berre, A. P., Fama, R., Sullivan, E. V. Executive Functions, Memory, and Social Cognitive Deficits and Recovery in Chronic Alcoholism: A Critical Review to Inform Future Research. *Alcoholism: Clinical and Experimental Research*. **41** (8), 1432-1443 (2017).
23. Marinkovic, K., Rickenbacher, E., Azma, S., Artsy, E. Acute alcohol intoxication impairs top-down regulation of Stroop incongruity as revealed by blood oxygen level-dependent functional magnetic resonance imaging. *Human Brain Mapping*. **33** (2), 319-333 (2012).
24. Marinkovic, K., Rickenbacher, E., Azma, S., Artsy, E., Lee, A. K. Effects of acute alcohol intoxication on saccadic conflict and error processing. *Psychopharmacology (Berl)*. **230** (3), 487-497 (2013).
25. Field, M., Wiers, R. W., Christiansen, P., Fillmore, M. T., Verster, J. C. Acute alcohol effects on inhibitory control and implicit cognition: implications for loss of control over drinking. *Alcoholism: Clinical and Experimental Research*. **34** (8), 1346-1352 (2010).
26. Fillmore, M. T. Drug abuse as a problem of impaired control: current approaches and findings. *Behavioral and Cognitive Neuroscience Reviews*. **2** (3), 179-197 (2003).
27. Hingson, R., Winter, M. Epidemiology and consequences of drinking and driving. *Alcohol Reseach & Health*. **27** (1), 63-78 (2003).
28. Selzer, M. L., Vinokur, A., Van Rooijen, L. A self-administered Short Michigan Alcoholism Screening Test (SMAST). *Journal of Studies on Alcohol*. **36** (1), 117-126 (1975).
29. Babor, T., Higgins-Biddle, J. S., Saunders, J. B., Monteiro, M. G. *AUDIT: The Alcohol use disorders identification test: Guidelines for use in primary care*. WHO: World Health Organization, Geneva, Switzerland (2001).
30. Rice, J. P. *et al*. Comparison of direct interview and family history diagnoses of alcohol dependence. *Alcoholism: Clinical and Experimental Research*. **19** (4), 1018-1023 (1995).
31. Eysenck, H. J., Eysenck, S. B. G. *Manual of the Eysenck Personality Questionnaire*. Hodder & Staughton (1975).
32. Eysenck, S. B., Eysenck, H. J. Impulsiveness and venturesomeness: their position in a dimensional system of personality description. *Psychological Reports*. **43** (3 Pt 2), 1247-1255 (1978).
33. Maltzman, I., Marinkovic, K. in *The Pharmacology of Alcohol and Alcohol Dependence*. (eds H. Begleiter & B. Kissin) 248-306 Oxford University Press (1996).
34. Martin, C. S., Earleywine, M., Musty, R. E., Perrine, M. W., Swift, R. M. Development and validation of the Biphasic Alcohol Effects Scale. *Alcoholism: Clinical and Experimental Research*. **17** (1), 140-146. (1993).
35. Liu, H., Tanaka, N., Stufflebeam, S., Ahlfors, S., Hamalainen, M. Functional Mapping with Simultaneous MEG and EEG. *Journal of Visualized Experiments*. 10.3791/1668 [pii] (40), (2010).
36. Lee, A. K., Larson, E., Maddox, R. K. Mapping cortical dynamics using simultaneous MEG/EEG and anatomically-constrained minimum-norm estimates: an auditory attention example. *Journal of Visualized Experiments*. 10.3791/4262 [pii] (68), e4262 (2012).
37. Balderston, N. L., Schultz, D. H., Baillet, S., Helmstetter, F. J. How to detect amygdala activity with magnetoencephalography using source imaging. *Journal of Visualized Experiments*. 10.3791/50212 (76), (2013).
38. Breslin, F. C., Kapur, B. M., Sobell, M. B., Cappell, H. Gender and alcohol dosing: a procedure for producing comparable breath alcohol curves for men and women. *Alcoholism: Clinical and Experimental Research*. **21** (5), 928-930 (1997).
39. Marinkovic, K., Cox, B., Reid, K., Halgren, E. Head position in the MEG helmet affects the sensitivity to anterior sources. *Neurology and Clinical Neurophysiology*. **2004**, 30 (2004).
40. Dale, A. M., Sereno, M. I. Improved localization of cortical activity by combining EEG and MEG with MRI cortical surface reconstruction: A linear approach. *Journal of Cognitive Neuroscience*. **5** 162-176 (1993).
41. Dale, A. M., Fischl, B., Sereno, M. I. Cortical surface-based analysis. I. Segmentation and surface reconstruction. *Neuroimage*. **9** (2), 179-194 (1999).
42. Fischl, B., Sereno, M. I., Dale, A. M. Cortical surface-based analysis. II: Inflation, flattening, and a surface-based coordinate system. *Neuroimage*. **9** (2), 195-207 (1999).
43. Gramfort, A., Papadopoulos, T., Olivi, E., Clerc, M. OpenMEEG: opensource software for quasistatic bioelectromagnetics. *Biomedical Engineering Online*. **9**, 45 (2010).
44. Kybic, J. *et al*. A common formalism for the integral formulations of the forward EEG problem. *IEEE Transactions on Medical Imaging*. **24** (1), 12-28 (2005).
45. Dale, A. M. *et al*. Dynamic statistical parametric mapping: combining fMRI and MEG for high-resolution imaging of cortical activity. *Neuron*. **26** (1), 55-67 (2000).
46. Marinkovic, K. Spatiotemporal dynamics of word processing in the human cortex. *The Neuroscientist*. **10** (2), 142-152 (2004).
47. Oostenveld, R., Fries, P., Maris, E., Schoffelen, J. M. FieldTrip: Open source software for advanced analysis of MEG, EEG, and invasive electrophysiological data. *Computational Intelligence and Neuroscience*. **2011**, 156869 (2011).
48. Delorme, A., Makeig, S. EEGLAB: An open source toolbox for analysis of single-trial EEG dynamics. *Journal of Neuroscience Methods*. **134**, 9-21 (2004).
49. Gramfort, A. *et al*. MNE software for processing MEG and EEG data. *Neuroimage*. **86**, 446-460 (2014).
50. Lin, F. H. *et al*. Spectral spatiotemporal imaging of cortical oscillations and interactions in the human brain. *Neuroimage*. **23** (2), 582-595 (2004).
51. Fischl, B., Sereno, M. I., Tootell, R. B., Dale, A. M. High-resolution intersubject averaging and a coordinate system for the cortical surface. *Human Brain Mapping*. **8** (4), 272-284 (1999).
52. Maris, E., Oostenveld, R. Nonparametric statistical testing of EEG- and MEG-data. *Journal of Neuroscience Methods*. **164** (1), 177-190 (2007).
53. Marinkovic, K. *et al*. Spatiotemporal dynamics of modality-specific and supramodal word processing. *Neuron*. **38** (3), 487-497 (2003).
54. Nachev, P. Cognition and medial frontal cortex in health and disease. *Current Opinion in Neurology*. **19** (6), 586-592 (2006).

55. Kennerley, S. W., Walton, M. E., Behrens, T. E., Buckley, M. J., Rushworth, M. F. Optimal decision making and the anterior cingulate cortex. *Nature Neuroscience*. **9** (7), 940-947 (2006).
56. Aron, A. R., Robbins, T. W., Poldrack, R. A. Inhibition and the right inferior frontal cortex: one decade on. *Trends in Cognitive Sciences*. **18** (4), 177-185 (2014).
57. Erika-Florence, M., Leech, R., Hampshire, A. A functional network perspective on response inhibition and attentional control. *Nature Communications*. **5**, 4073 (2014).
58. D'Esposito, M., Postle, B. R. The cognitive neuroscience of working memory. *Annual Review of Psychology*. **66** 115-142 (2015).
59. Hasselmo, M. E., Stern, C. E. Theta rhythm and the encoding and retrieval of space and time. *Neuroimage*. **85 Pt 2**, 656-666 (2014).
60. Womelsdorf, T., Johnston, K., Vinck, M., Everling, S. Theta-activity in anterior cingulate cortex predicts task rules and their adjustments following errors. *Proceedings of the National Academy of Sciences of the United States of America*. **107** (11), 5248-5253 (2010).
61. Fries, P. A mechanism for cognitive dynamics: neuronal communication through neuronal coherence. *Trends in Cognitive Sciences*. **9** (10), 474-480 (2005).
62. Canolty, R. T. *et al.* High gamma power is phase-locked to theta oscillations in human neocortex. *Science*. **313** (5793), 1626-1628 (2006).
63. Varela, F., Lachaux, J. P., Rodriguez, E., Martinerie, J. The brainweb: phase synchronization and large-scale integration. *Nature Reviews Neuroscience*. **2** (4), 229-239 (2001).
64. Hanslmayr, S. *et al.* The electrophysiological dynamics of interference during the Stroop task. *Journal of Cognitive Neuroscience*. **20** (2), 215-225 (2008).
65. Niendam, T. A. *et al.* Meta-analytic evidence for a superordinate cognitive control network subserving diverse executive functions. *Cognitive, Affective, & Behavioral Neuroscience*. **12** (2), 241-268 (2012).
66. Sadaghiani, S., D'Esposito, M. Functional Characterization of the Cingulo-Opercular Network in the Maintenance of Tonic Alertness. *Cerebral Cortex*. **25** (9), 2763-2773 (2015).
67. Dosenbach, N. U., Fair, D. A., Cohen, A. L., Schlaggar, B. L., Petersen, S. E. A dual-networks architecture of top-down control. *Trends in Cognitive Sciences*. **12** (3), 99-105 (2008).
68. Bullmore, E., Sporns, O. The economy of brain network organization. *Nature Reviews Neuroscience*. **13** (5), 336-349 (2012).
69. Fornito, A., Zalesky, A., Breakspear, M. The connectomics of brain disorders. *Nature Reviews Neuroscience*. **16** (3), 159-172 (2015).
70. Anderson, B. M. *et al.* Functional imaging of cognitive control during acute alcohol intoxication. *Alcoholism: Clinical and Experimental Research*. **35** (1), 156-165 (2011).
71. Kareken, D. A. *et al.* Family history of alcoholism interacts with alcohol to affect brain regions involved in behavioral inhibition. *Psychopharmacology (Berl)*. **228** (2), 335-345 (2013).
72. Schuckit, M. A. *et al.* fMRI differences between subjects with low and high responses to alcohol during a stop signal task. *Alcoholism: Clinical and Experimental Research*. **36** (1), 130-140 (2012).
73. Nikolaou, K., Critchley, H., Duka, T. Alcohol affects neuronal substrates of response inhibition but not of perceptual processing of stimuli signalling a stop response. *PLoS One*. **8** (9), e76649 (2013).
74. Gan, G. *et al.* Alcohol-induced impairment of inhibitory control is linked to attenuated brain responses in right fronto-temporal cortex. *Biology Psychiatry*. **76** (9), 698-707 (2014).
75. Ehlers, C. L., Wills, D. N., Havstad, J. Ethanol reduces the phase locking of neural activity in human and rodent brain. *Brain Research*. **1450**, 67-79 (2012).
76. Goldstein, R. Z., Volkow, N. D. Dysfunction of the prefrontal cortex in addiction: neuroimaging findings and clinical implications. *Nature Reviews Neuroscience*. **12** (11), 652-669 (2011).